The structure of the unidirectionally solidified Al–$Al_{21}Pt_5$ eutectic alloys

The Al–Pt phase diagram displays a eutectic on the aluminium side, but the exact location of the eutectic point is uncertain. Two markedly different compositions are reported in the literature, namely 7 wt % Pt at 930 K [1] and 3.1 wt % Pt at 928.6 K [2]. The phase in equilibrium with aluminium is Al_4Pt (64.3 wt % Pt) or more probably $Al_{21}Pt_5$ according to [3]. This latter is cubic (lattice parameter $a = 19.226 \times 10^{-10}$ m) and is formed by peritectic reaction at 1080 K from Al_3Pt (73.3 wt % Pt) [1]. The results of a study of the structure of this as yet not defined eutectic are reported here. In this study a wide range of solidification conditions and compositions has been investigated.

Different alloys with nominal compositions between 4.0 and 10.0 wt % Pt were prepared starting from slightly impure elements (99.99 Al and 99.98 Pt) by induction furnace melting in Al_2O_3 crucibles under argon, and casting into graphite moulds. The resulting ingots were remelted and unidirectionally solidified in a vertical tube furnace at growth rates (R) ranging from 2.8×10^{-4} to 1.23×10^{-2} cm sec^{-1} under a thermal gradient (G) of the order of 100° C cm^{-1}. The equipment has already been described in detail elsewhere [4]. Sections normal and parallel to the growth axis were examined after diamond polishing and etching in aqueous solution ($\frac{1}{3}$ HNO_3 + $\frac{2}{3}$ H_2O) for 2 to 5 sec at 3 V. Chemical analyses were also performed on suitable samples taken from the middle zone of the unidirectionally solidified ingots.

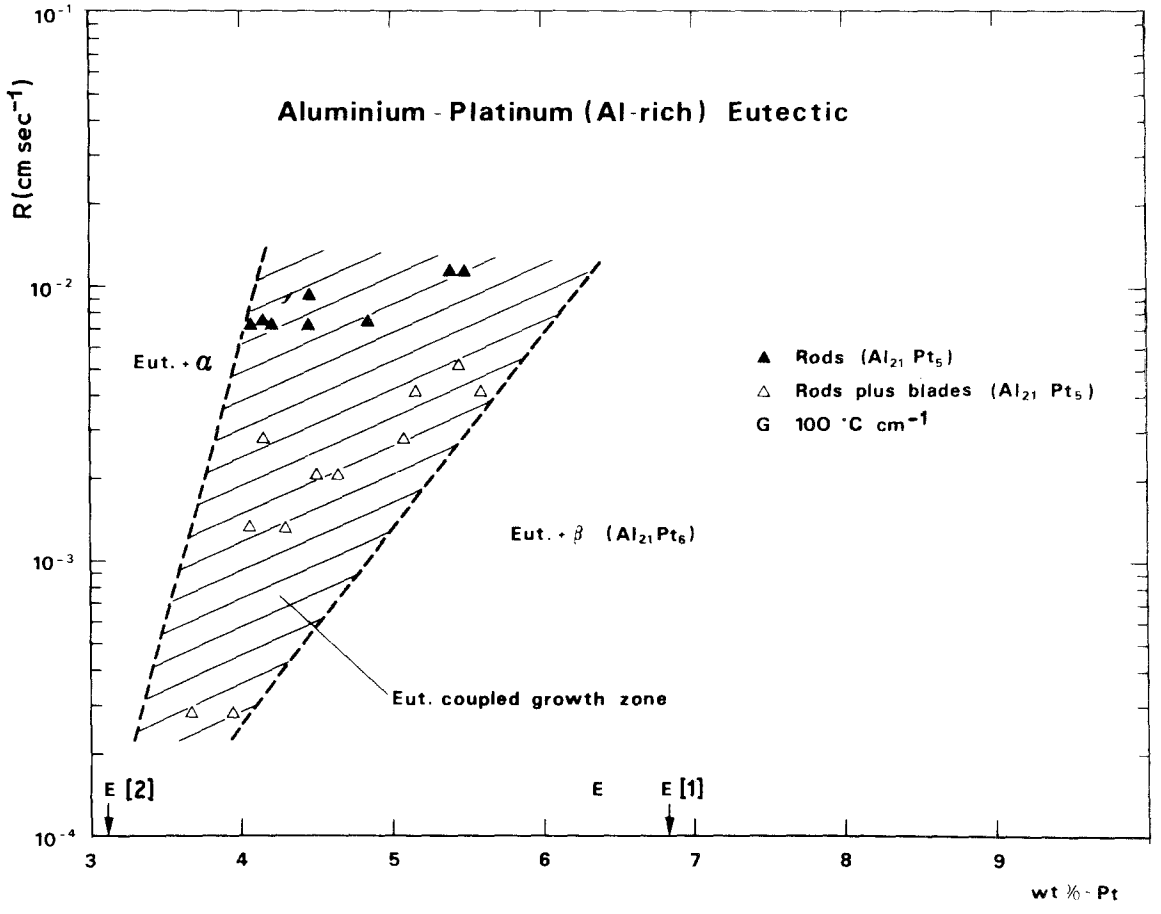

Figure 1 Growth rate versus alloy composition showing the range of the coupled growth region for Al–Pt alloys. The eutectic points (E) reported in the literature [1–2] are indicated.

0022–2461/80/092403–06$02.60/0

The results in Fig. 1, in which the growth rate is plotted against alloy composition, shows the existence of a coupled zone over the range 3.8 to 5.5 wt% Pt which seems to endorse the value of 3.1 wt% Pt [2] as the more correct location of the eutectic point. Outside this range, in which eutectic structures grown, dendrites (primary α or β) plus eutectic are formed. The zone of coupled growth is skewed toward the hypereutectic composition as in the case of other systems, such as Al–Ni and Al–Co [5]. The experimental points concerning hypoeutectic and hypereutectic structure were not plotted in the figure because the chemical analysis has revealed a strong segregation due to the appreciable difference in density between Al and the second phase ($\Delta d \simeq 3000\,\mathrm{kg\,m^{-3}}$). Strong segregation phenomena were observed earlier in other eutectics namely in Al–Al_4U [6] and Al–Al_2Au [7].

The fully eutectic compositions of the thermal gradient coupled growth zone are characterized by a rod composite morphology, as is clearly illustrated by the micrographs of transverse sections (Fig. 2). The rods are generally aligned and parallel to each other (Fig. 2a), but in some areas the presence of misaligned rods near to aligned ones (Fig. 2b) is observed. The rods are also parallel to the direction of growth (normal to the plane of Fig. 2a and b). With decreasing R there is a gradual rods → blades transition. Below a value of $R = 6 \times 10^{-3}\,\mathrm{cm\,sec^{-1}}$

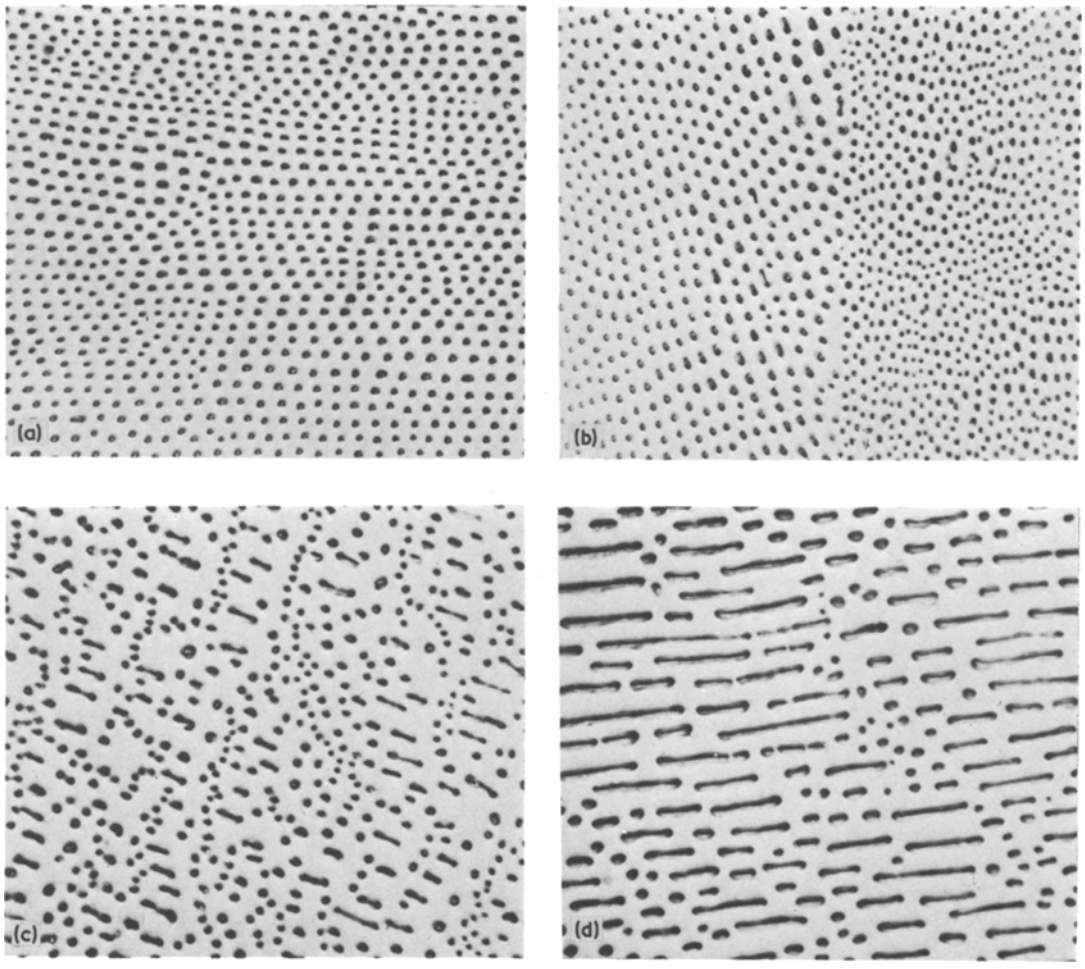

Figure 2 Optical micrographs (transverse sections) showing variation of eutectic micromorphology with growth rates: (a) $R = 7.50 \times 10^{-3}\,\mathrm{cm\,sec^{-1}}$; (b) $R = 7.50 \times 10^{-3}\,\mathrm{cm\,sec^{-1}}$; (c) $R = 3.19 \times 10^{-3}\,\mathrm{cm\,sec^{-1}}$; (d) $R = 2.78 \times 10^{-3}\,\mathrm{cm\,sec^{-1}}$; × 1000.

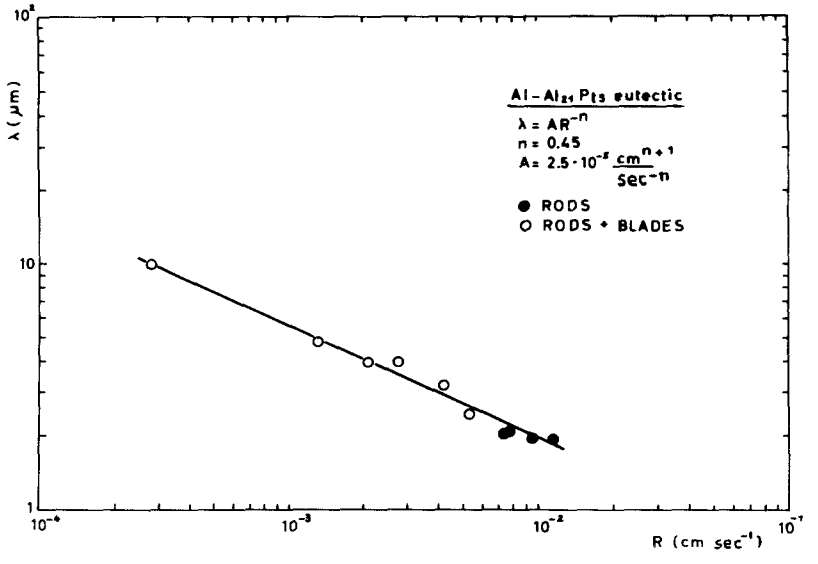

Figure 3 Plot of measured interparticle spacing, λ, versus growth rate, R.

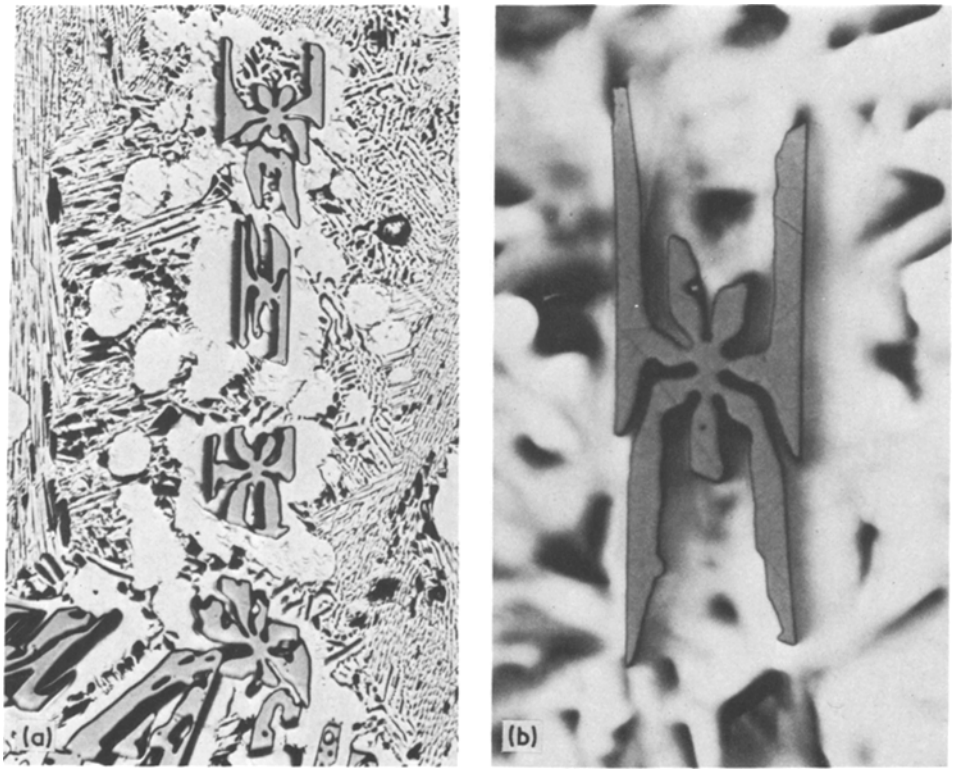

Figure 4 Optical micrographs showing hypereutectic micromorphology (Al plus primary $Al_{21}Pt_6$). (a) $R = 1.23 \times 10^{-2}$ cm sec^{-1}, × 200; (b) $R = 7.50 \times 10^{-3}$ cm sec^{-1}, unetched sample, × 1000.

the morphology consists of a mixture of blades and rods in small groups (Fig. 2c) whereas in some areas of the specimens a blade morphology following parallel arrays is predominant (Fig. 2d). The nature of the second phase (rods and blades) coexisting with Al in eutectic structure has been investigated by X-ray diffractometry using Cu$K\alpha$ radiation, on powdered specimens obtained after extraction of the phase from the matrix by electrochemical etching. The phase corresponds to the intermetallic compound $Al_{21}Pt_5$ of cubic symmetry and with a unit cell parameter of 19.32×10^{-10} m, which is slightly greater than that reported in the literature [3]. The phase Al_4Pt has not been found. Moreover, the dependence of the interphase spacing, λ, on the growth rate has been determined for the coupled growth alloys using the intercept method on transverse sections. The well known relationship $\lambda = A \cdot R^{-n}$ [8] has been found to be valid over the whole range of growth rates investigated (Fig. 3). A further point worth noting (from a macromorphological point of view) is the presence of colony structures at high growth rates ($R > 5 \times 10^{-3}$ cm sec^{-1}).

According to the generally accepted rule of the volume ratio [9] a eutectic has a fibrous or a lamellar structure depending on whether the volume fraction of the reinforcing phase is lower or higher than 30%. In the Al–$Al_{21}Pt_5$ system (5.31 vol% second phase according to author's calculations) a fibrous structure is formed which is predictable by the rule of the volume ratio. At very low growth rates the $Al_{21}Pt_5$ grows also in lamellae (blades). A similar behaviour is reported in the Al–Al_3Ni system [10]. Colonies form in an impure alloy when the solidification rates are high [11].

In hypereutectic structures, the primary β phase is present in two morphologically distinct crystal habits depending on the solidification parameters. Dendritic crystals are preferentially obtained at high solidification rates, while at lower rates large irregular crystals are formed. The micromorphology shown in Fig. 4a presents dendritic primary crystals surrounded by an Al halo acting as a bridge between dendrites and interdendritic eutectic. The dendritic form is clearly visible in Figs. 4b and 5a. The latter is a scanning electron micrograph after a deep etching of the Al matrix. The large irregular crystals as well as the dendrites have been electrolytically extracted from the matrix (Fig. 5b). These were large enough to be

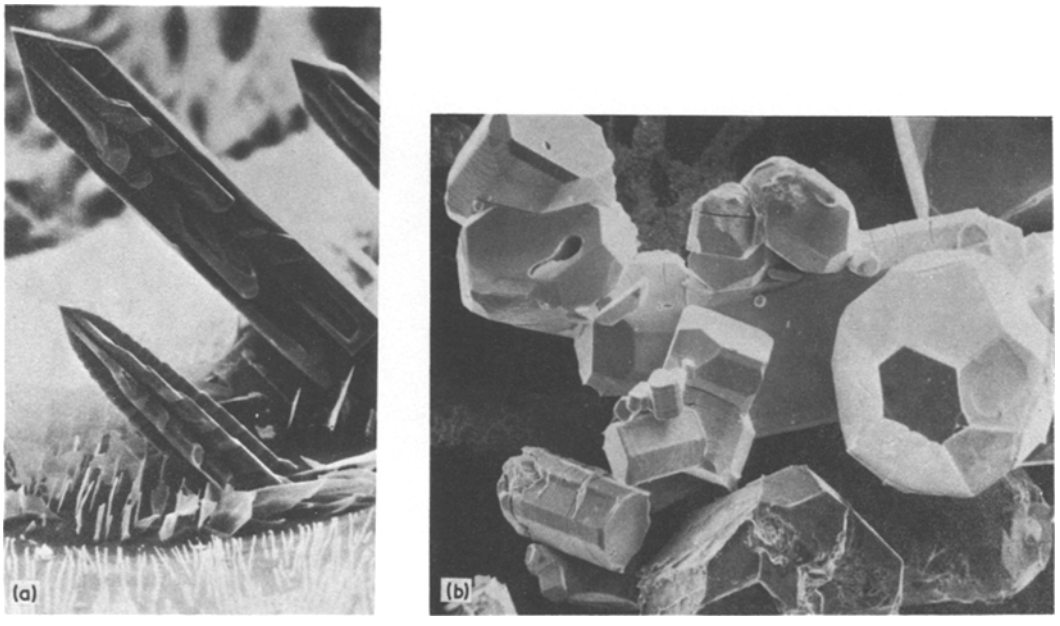

Figure 5 $Al_{21}Pt_6$ crystal morphology. (a) Faceted dendrites formed at high solidification rate brought out by a deep electrochemical etching of the Al matrix, × 500. (b) Irregular crystals formed at low solidification rate obtained by complete dissolution of Al matrix (electrochemical etching) × 500.

TABLE I Observed and calculated d_{hkl} values of the metastable phase $Al_{21}Pt_6$. Structure: hexagonal, $a = 13.02$ Å, $c = 9.61$ Å, $c/a = 0.7381$

$h\,k\,l$	I/I_0	d_{obs} (Å)	d_{calc} (Å)
0 0 1	1	9.61	9.610
2 0 1	2	4.86	4.863
0 0 2	45	4.81	4.805
2 1 0	2	4.27	4.262
2 1 1	2	3.90	3.896
3 0 0	66	3.754	3.758
3 0 2	100	2.958	2.960
3 1 1			2.973
2 2 2	2	2.698	2.694
4 1 0	2	2.465	2.460
0 0 4	16	2.398	2.402
4 1 1	9	2.389	2.383
2 2 3	10	2.286	2.283
1 1 4	3	2.255	2.255
3 1 3	6	2.239	2.237
4 1 2	6	2.195	2.195
5 0 1			2.190
3 3 0	60	2.174	2.170
2 1 4	6	2.092	2.092
4 2 1	7	2.085	2.080
5 0 2	18	2.032	2.041
3 0 4	64	2.026	2.024
5 1 0			2.025
3 3 2	58	1.979	1.977
4 1 3	3	1.955	1.951
6 0 0	14	1.883	1.880
4 3 1	25	1.815	1.819
2 1 5	17	1.754	1.752
6 0 2			1.750
3 3 4	6	1.613	1.610
4 3 3	7	1.603	1.604
4 4 1			1.604
1 1 6	1	1.560	1.555
6 0 4	14	1.482	1.480
6 2 2			1.487
4 3 4	5	1.468	1.467
3 1 6	4	1.424	1.424
6 3 0			1.420
6 3 2	44	1.365	1.362
3 2 6			1.361
6 0 5	5	1.350	1.343
5 4 3	2	1.318	1.316
5 0 6	2	1.310	1.310
6 3 3	6	1.293	1.293
3 3 6	4	1.288	1.288
5 1 6	4	1.255	1.256
5 5 2			1.256
5 3 5	22	1.226	1.230
6 3 4	12	1.220	1.222
6 0 6	10	1.215	1.218
6 4 3	7	1.202	1.199
0 0 8			1.198
4 4 6	10	1.145	1.142
6 3 5			1.141
6 2 6	2	1.113	1.118
6 6 0	7	1.088	1.085
6 6 1	4	1.077	1.078
Follow 10 other lines			

analysed separately by X-rays on a Weissenberg camera and successively for their chemical composition and density. Both the dendritic type as well as the large irregular crystals gave similar X-ray diffraction patterns, but no familiar intermediate phase could be identified in these patterns [4, 12–14].

Fifty-five diffraction lines were observed and after several trial-and-error procedures the best indexing was obtained by assuming a hexagonal cell with parameters $a = 13.02$ Å, $c = 9.61$ Å, $c/a = 0.738$. Observed and calculated d values are listed in Table I. The chemical analysis gave 66.8 wt % Pt and 32.9 wt % Al which corresponds to the empirical formula $Al_{3.56}Pt$. The average density as determined by the pycnometer and hydrostatic balance methods is 6250 kg m^{-3}. The total number of atoms per unit cell, as calculated from density and chemical analysis data is 82 (64 Al atoms and 18 Pt atoms). The chemical formula of the phase is thus $Al_{21}Pt_6$, while the number of formula weights per unit cell is three.

It can be postulated that $Al_{21}Pt_6$ is a metastable phase. In fact the X-ray analysis after heat treatment for several hours at 200° C shows that the $Al_{21}Pt_6$-phase transforms slowly into $Al_{21}Pt_5$, the phase in equilibrium with Al at the eutectic composition. A compound suppression and formation of new and different compounds can occur in eutectic systems. An example is found in the Al–Fe eutectic which presents a stable compound Al_3Fe and a metastable Al_6Fe depending on solidification conditions [15].

Acknowledgements

The authors wish to thank Messrs E. Haine, A. Misirocchi and F. Quazzo for the technical assistance in performing the experiments. Thanks are also due to Dr G. Serrini for his advice and support in the chemical analysis work.

References

1. R. HUCH and W. KLEMM, *Z. Anorg. Allgem. Chem.* **329** (1964) 123.

2. E. H. WRIGHT *et al.*, Alcoa Res. Labs. Tech. Pap. 15 (1960).
3. L. F. MONDOLFO, "Aluminium Alloys: Structure and Properties" (Butterworths, London, 1976).
4. K. N. STREET, C. F. ST JOHN and G. PIATTI, *J. Inst. Metals* **95** (1967) 326.
5. R. S. BARKLAY, H. W. KERR and P. NIESSEN, *J. Mater. Sci.* **6** (1971) 1168.
6. B. CHALMERS, "Principles of Solidification" (Wiley, New York, 1964).
7. G. PIATTI and G. PELLEGRINI, *J. Mater. Sci.* **11** (1976) 913.
8. W. A. TILLER, "Liquid Metals and Solification" (A.S.M., Cleveland, Ohio, 1958).
9. L. M. HOGAN, R. W. KRAFT and F. D. LEMKEY, "Advances in Materials Research", Vol. 5, edited by H. Herman (Wiley, New York, 1971).
10. F. D. LEMKEY, R. W. HERTZBERG and J. A. FORD, *Trans. AIME* **233** (1965) 334.
11. H. W. WEART and D. J. MACK, *ibid.* **212** (1958) 664.
12. L. E. EDSHAMMAR, *Acta Chem. Scand.* **20** (1966) 2863.
13. M. TONJEC, A. TONJEC and A. BONEFACIC, *J. Mater. Sci.* **9** (1974) 523.
14. F. A. SHUNK, "Constitution of Binary Alloys", Secondary Supplement (McGraw-Hill, New York, 1969).
15. C. McL. ADAM and L. M. HOGAN, *J. Aust. Inst. Metals* **16** (1972).

Received 21 December 1979
and accepted 18 January 1980

G. PIATTI
G. PELLEGRINI
Materials Science Division,
Joint Research Centre,
21020 ISPRA (Va),
Italy